ICAS-88-3.2.4

REAL-TIME GUIDANCE LAWS FOR THREE-DIMENSIONAL INTERCEPTION

M. Do Khac and H.T. Huynh
Office National d'Etudes et de Recherches Aérospatiales
Châtillon, France

Abstract

Quasi-optimal real-time feedback guidance laws have been developed for three-dimensional minimum-time interception of a fighter aircraft. The technique used is derived from singular perturbation theory (SPT) with a realistic time-scale separation between different state variables. Two feedback control laws have been developed. They are based on two sets of the state variables.

In the first one, the state vector is split in four distinct time scales, namely in order of increasing speed: horizontal relative position x and y, specific energy E, azimuth angle χ, altitude h and flight path angle γ. A linearization of the dynamic equations associated with the fastest variables h and γ, used in conjonction with the reset technique, allows a feedback control law, uniformly valid in the whole flight envelope for a three-dimensional interception.

In the second one, the same time-scale decomposition as above is used, but the state variable E is replaced by the kinematic velocity V. In order to improve the accuracy of the final interception, where the SPT fails, different techniques are then proposed.

The obtained control laws are of closed-loop type and can fulfil terminal constraints on interceptor-target distance.

Three sets of three-dimensional interception examples covering the whole range of azimuth angle χ and a large range of speed V and altitude h have been computed by the two above methods.

Numerical results have been compared with the exact open-loop optimal control solutions obtained by a projected-gradient optimization algorithm.

The trajectories provided by real-time guidance control laws are slightly less accurate than the optimal ones, but the computation times are very small and are compatible with real-time on-board computer applications.

1. Introduction

An improvement of the performance management could be obtained for combat aircraft by computing optimal guidance laws, in real-time on-board computers. The flight path optimization involves non-linear optimal control, and the exact solutions are only available by using non-linear programming techniques which require a large amount of calculations, and so are not suited for on-board real-time computation of optimal flight paths. For this reason, research in quasi-optimal flight path, with reduced time-consuming computations, remain an interesting domain for investigation.

The present paper is concerned with the three-dimensional interception manoeuvers. Although this subject has required the attention of many studies, quasi-optimal guidance laws,uniformly valid for the whole flight envelope, with low computational cost, have not been available up to now.

Among the various approximations techniques, the singular perturbation theory (SPT)[10] has been used successfully and provides simplified control laws, in a closed-loop form, suitable with on-board real time computation[1-7]. Nevertheless, few comparisons have been made with the "exact" optimal solutions in order to quantify the accuracy of the obtained solutions[5,7]. In a previous study[7], an application of SPT, based on a realistic time-scale decomposition, has provided guidance laws for vertical interception trajectories. Comparison with exact open-loop optimal solutions, derived from an iterative numerical method based upon a projected gradient technique, has shown the quasi-optimality of the obtained guidance laws, a better than 1% accuracy has been achieved for the performance index. Moreover, those guidance laws were uniformly valid for the whole flight envelope and were suitable for on-board computers.

The objective of this paper is to extend the previous technique, based on SPT, in order to develop quasi-optimal guidance laws for three-dimensional mimimum time interception and for on-board computer application, and valid for a large flight envelope. Two control laws, of closed-loop type, are derived from two sets of state variables, by using a realistic time-scale decomposition. A general approach is proposed in order to improve the accuracy of the final interception, where the SPT fails.

The approximate solutions are then compared in numerical simulations with the exact ones provided by a numerical gradient technique.

2. Optimal aircraft trajectory formulation

The aircraft is assumed as a point mass model, constant mass, and the motion is referenced to an inertial frame in a flat earth with constant gravity.

The state variables of the aircraft are the horizontal coordinates centered at the target airplane x and y, the aircraft velocity V or the specific energy E defined as $E = h + V^2/2g$, the path azimuth angle χ, the altitude h and the flight path angle γ. The control laws are developed with the assumption that the target is flying with constant velocity V_T at constant altitude h_T.

The thrust F is directed along the flight path with the maximum value F_M given in a two-dimensional table $F_M(h,M)$. The aerodynamic polar is assumed to have conventional parabolic form: $C_x = C_{x0} + k\ C_z^2$ where C_{x0} and k are tabulated functions of the Mach number M.

The control variables are the load factor n_z defined as $n_z = q\ S\ C_z/mg$, where $q = \rho\ V^2/2$ is the dynamic pressure, and the bank angle μ. For interception trajectories considered in this paper, thrust is assumed to be always set at its maximum value F_M.

In the following, dimensionless variables will be used:
$\bar{t}=gt/a_0$, $\bar{x}=gx/a_0^2$, $\bar{y}=gy/a_0^2$, $\bar{h}=gh/a_0^2$, $\bar{V}=V/a_0$, $\bar{F}_m=F_M/mg$, $\bar{E}=Eg/a_0^2$, where a_0 is a reference sonic velocity. Dropping the symbol $(\bar{\cdot})$ for simplification, the aircraft equations of motion are given by:

$$
\begin{aligned}
&(1a)\quad \dot{x} = V\cos\gamma\cos\chi - V_T\\
&(1b)\quad \dot{y} = V\cos\gamma\sin\chi\\
&(1c)\quad \dot{E} = V(F_M - D_0 - D_1 n_z^2)\\
&(1d)\quad \dot{\chi} = n_z \sin\mu / V\cos\gamma\\
&(1e)\quad \dot{h} = V\sin\gamma\\
&(1f)\quad \dot{\gamma} = (n_z\cos\mu - \cos\gamma)/V
\end{aligned}
\qquad (1)
$$

with
$$
\begin{aligned}
D_0 &= q\,S\,C_{x0}/mg\\
D_1 &= k\,mg/q\,S.
\end{aligned}
$$

Using the velocity V instead of specific energy E, we have the same equations of motion, except that the third equation of (1) is replaced by:

$$(1c')\quad \dot{V} = F_M - D_0 - D_1 n_z^2 - \sin\gamma$$

The problem consists to find the optimal control laws n_z, μ in order to minimize the performance index:

$$J = \int_0^{t_f} dt = t_f \qquad (2)$$

subject to the following state and control constraints:

$$
\begin{aligned}
&C_{z\,min} \le C_z \le C_{z\,max}\\
&n_{z\,min} \le n_z \le n_{z\,max}\\
&q = \rho V^2/2 \le q_{max}\\
&M \le M_{max}
\end{aligned}
\qquad (3)
$$

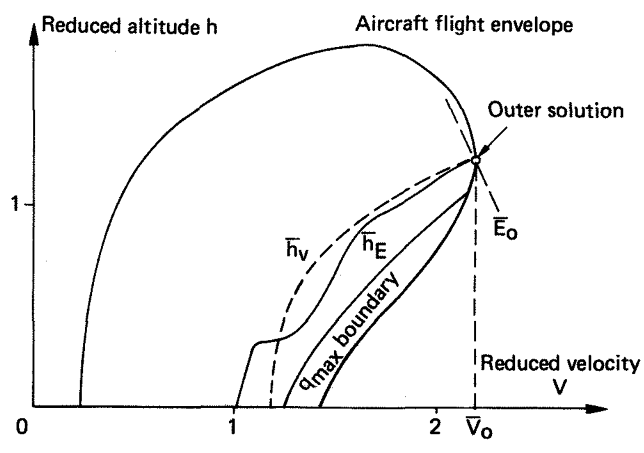

Fig. 1 - Energy-climb profile $\bar{h}_E$ and velocity-climb profile $\bar{h}_V$ for minimum-time interception.

The initial state vector of the aircraft is fully specified, and for interception problem, the final requirements are:

$$x(t_f) = 0,\quad y(t_f) = 0,\quad h(t_f) = h_T \qquad (4)$$

A typical combat aircraft model, with high performance level, will be used in numerical applications. The flight envelope of the model is given in Fig. 1.

3. General outline of guidance law computation

3.1. Singularly perturbed optimal control problem

In what follows, SPT is applied to two sets of state variables: the first set uses the state variables as described by equations (1), the second one uses almost the same set, with the exception that the specific energy E is replaced by velocity V.

For the first set, the equations of motion (1) are written in the following singularly perturbed form:

$$
\begin{aligned}
\dot{x} &= V\cos\gamma\cos\chi - V_T\\
\dot{y} &= V\cos\gamma\sin\chi\\
\varepsilon\,\dot{E} &= V(F_m - D_0 - D_1 n_z^2)\\
\varepsilon^2\,\dot{\chi} &= n_z\sin\mu/V\cos\gamma\\
\varepsilon^3\,\dot{h} &= V\sin\gamma\\
\varepsilon^3\,\dot{\gamma} &= (mg\cos\mu - \cos\gamma)/V
\end{aligned}
\qquad (5)
$$

where ε is a "small" parameter which is artificially introduced to separate the time-scales between the state variables.

In this form, the aircraft dynamic is thus ordered in four time-scales, respectively from the slowest to the fastest one as follows: the relative horizontal coordinates x and y, specific energy E, azimuth angle χ, altitude h and flight path angle γ.

For the second set, the same time-scale decomposition is considered, and the equations of motion, in a singularly perturbed form, are:

$$
\begin{aligned}
\dot{x} &= V\cos\gamma\cos\chi - V_T\\
\dot{y} &= V\cos\gamma\sin\chi\\
\varepsilon\,\dot{V} &= F_m - D_0 - D_1 n_z^2 - \sin\gamma\\
\varepsilon\,\dot{\chi} &= n_z\sin\mu/V\cos\gamma\\
\varepsilon^3\,\dot{h} &= V\sin\gamma\\
\varepsilon^3\,\dot{\gamma} &= (n_z\cos\mu - \cos\gamma)/V
\end{aligned}
\qquad (6)
$$

In the following, the method is described only for the first set of state variables, the application to the second one can be done straightforwardly.

To solve the optimal control problem defined by (2) (3) (4) (5), the Hamiltonian is formed (by neglecting terms taken into account the constraints on state variables and on controls (3)):

$$
\begin{aligned}
H = 1 &+ \lambda_x(V\cos\gamma\cos\chi - V_T) + \lambda_y V\cos\gamma\sin\chi \ldots\\
&\ldots + \lambda_E V(F_m - D_0 - D_1 n_z^2) + \lambda_\chi n_z\sin\mu/V\cos\gamma \ldots\\
&\ldots + \lambda_h V\sin\gamma + \lambda_\gamma (n_z\cos\mu - \cos\gamma)/V
\end{aligned}
\qquad (7)
$$

where the adjoint variables λ_x, λ_y, λ_E, λ_χ, λ_h, λ_γ are given by the differential equations:

$$
\begin{aligned}
\dot{\lambda}_x &= -\partial H/\partial x = 0 & & \lambda_{x_F} = v_x\\
\dot{\lambda}_y &= -\partial H/\partial y = 0 & & \lambda_{y_F} = v_y\\
\varepsilon\,\dot{\lambda}_E &= -\partial H/\partial E|_h & \text{with}\quad & \lambda_{E_F} = 0\\
\varepsilon^2\,\dot{\lambda}_\chi &= -\partial H/\partial \chi & & \lambda_{\chi_F} = 0\\
\varepsilon^3\,\dot{\lambda}_h &= -\partial H/\partial h|_E & & \lambda_{h_F} = v_h\\
\varepsilon^3\,\dot{\lambda}_\gamma &= -\partial H/\partial \gamma & & \lambda_{\gamma_F} = 0
\end{aligned}
\qquad (8)
$$

where v_x, v_y and v_h are arbitrary constants.

The optimal control laws (n_z^*, μ^*) must be chosen in order to minimize the Hamiltonian (7), that is:

$$(n_z^*, \mu^*) = Arg \underset{(n_z,\mu)}{Min} \quad H(X, \lambda, n_z, \mu) \tag{9}$$

where X is the state vector, λ the adjoint vector, with components: $X = [x,y,E,\chi,h,\gamma]$, $\lambda = [\lambda_x,\lambda_y,\lambda_E,\lambda_\chi,\lambda_h,\lambda_\gamma]$.

Let us notice that the Hamiltonian, along a optimal trajectory, is identically equal to zero:

$$H(X^*, \lambda^*, n_z^*, \mu^*) \equiv 0$$

This property is used to derive optimal solution in the singular perturbation approximation technique.

3.2. General outline of the method

In order to obtain approximate guidance laws, of closed-loop type, and valid for a large flight envelope, it is necessary to modify the original zeroth-order solution derived from SPT, by adding corrections based upon considerations about first-order approximations.

A complete guidance law is obtained by using the following steps:

i) Computation of zeroth-order solution by SPT,
ii) Closed-loop control law for "initial" and "outer" solution,
iii) Final control law,
iv) First-order corrections.

i) Zeroth-order solution by SPT

A zeroth-order solution of the singularly optimal control problem, given by (5) (7) (8) (9), is obtained by solving firstly the reduced problem which is defined by setting $\varepsilon=0$ in equations (5) and (8). The so-obtained solution is called outer solution, or reduced-order solution. This outer solution introduces discontinuities on initial and final conditions on the "fast" variables, that is on E, χ, h and γ. The "matching" on these variables is obtained by introducing three successive "boundary-layers", each of which is related to a time-scale among the fast variables. A composite control law, uniformly valid from initial time to final time of interception, can be obtained by a superposition of the control laws obtained from reduced-order solution and "boundary-layers" solutions.

Thus, a typical composite control law $u_{CP}(t)$ can be written in the following form:

$$u_{CP}(t) = \sum_{i=1}^{3} \hat{u}_i(X(\tau_i),\tau_i) + \bar{u}(X(t)) + \sum_{i=1}^{3} \tilde{u}_i(X(\sigma_i),\sigma_i) \tag{10}$$

The used symbols in this equation have the following meaning: $u=[\mu,n_z]$, X is the state vector, the subscript i is related to the ith "boundary-layer", τ_i and σ_i use the transformation variables related to the corresponding boundary-layer ($\tau_i = (t-t_0)/\varepsilon^i$, $\sigma_i = (t_f-t)/\varepsilon^i$, the symbol $\hat{u}$ is related to the initial boundary-layer, $\tilde{u}$ is related to final boundary-layer, $\bar{u}$ is related to the outer solution.

The "boundary-layers" controls $\hat{u}_i$ and $\tilde{u}_i$ satisfy, in principle, the following asymptotic convergence properties:

$$\begin{aligned} &\lim_{\tau_i \to \infty} \quad \hat{u}_i(X(\tau_i),\tau_i) = \bar{u}(X(t_o)) \\ &\lim_{\sigma_i \to \infty} \quad \tilde{u}_i(X(\sigma_i),\sigma_i) = \bar{u}(X(t_f)) \end{aligned} \tag{11}$$

ii) Initial and "outer" control law

A closed-loop control law is obtained by noticing that, at initial time $t=t_0$, the "final boundary" controls $u_i(X(\sigma_i),\sigma_i)$ are neglectable and the control is given by the innest boundary-layer term, that is:

$$u_{CP}(t_0) \simeq \hat{u}_3(X_0) \tag{12}$$

where $\hat{u}_3(X_0)$ is, for the case in study, the control related to the boundary-layer equations on altitude and flight-path angle.

Thus, by replacing the initial state by the current state $X(t)$, we obtain a closed-loop control law which is uniformly valid along the flight path, with the exception of a neighbourhood of the final conditions. The reason for this simplification stems from the asymptotic convergence properties of the boundary-layers controls, given by (11). This control is named "reset" control.

iii) Final control law

At the vicinity of the final conditions, the above control law is no more suitable, and the final boundary-layer control, given by the last terms in (10) should be used, in order to achieve final desired conditions. Nevertheless, as the final "boundary-layers" controls are asymptotically stable in inverse time, their application in direct-time would provide inaccurate final conditions.

A particular technique is suggested in order to circumvent this problem.

iv) First-order corrections

Finally, improvements of the closed-loop guidance laws can be obtained by taking into account some first-order correction terms.

A more detailed derivation of the guidance laws, in a closed loop form, is described below.

4. Closed-loop control law for three-dimensional interception

4.1. Zeroth-order control laws

Until further notice, the following statement is available for the two previous state variable sets.

4.1.1. Outer solution

The reduced-order solution, obtained by setting $\varepsilon=0$ in (5) (8) is given by:

$$\begin{aligned} &\bar{V}_o = V_{\max} \\ &\bar{h}_o, \bar{E}_o = arg \underset{h,E}{max}(V) \quad \text{with} \quad F_m - D_o - D_1 = 0 \\ &\bar{\chi}_o = \psi - sin^{-1}(V_T sin\,\psi / \bar{V}_o) \\ &\bar{\gamma}_o = 0, \ \bar{n}_{zo} = 1, \ \bar{\mu}_o = 0 \\ &\bar{\lambda}_{xo} = cos\,\bar{\chi}_o / (V_T cos\,\bar{\chi}_o - \bar{V}_o) \\ &\bar{\lambda}_{yo} = sin\,\bar{\chi}_o / (V_T cos\,\bar{\chi}_o - \bar{V}_o) \end{aligned} \tag{13}$$

where $\psi = tan^{-1}(y/x)$ is the horizontal projection of the line-of-sight angle (Fig 2).

The outer solution is defined by a point in the (h,V) diagram (Fig 1) and corresponds to a level flight at maximum speed $\bar{V}_0 = V_{max}$. In horizontal projection, the "outer solution" is a "collision" trajectory type (see Fig 2).

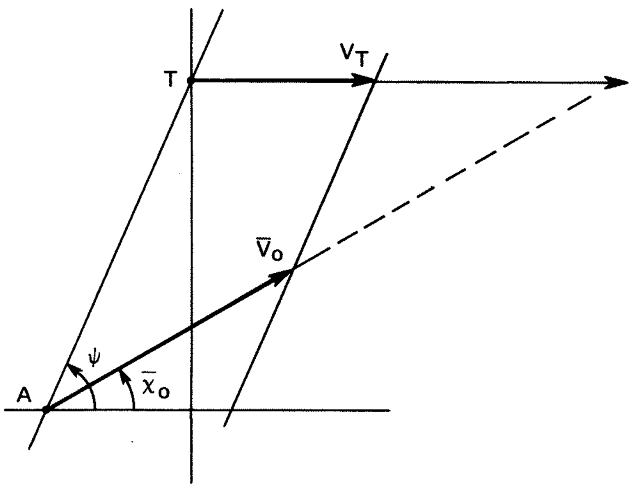

Fig.2a - Outer solution illustration.

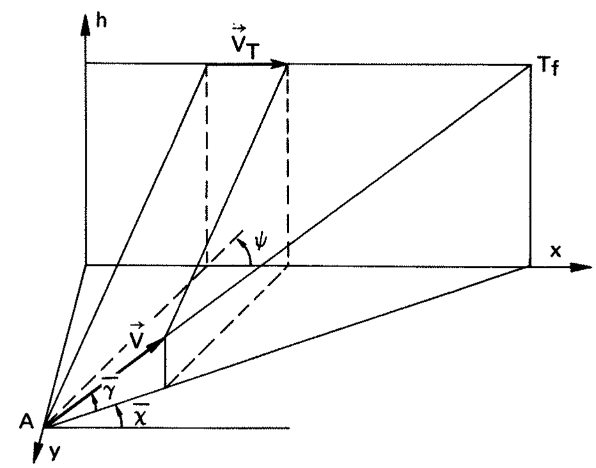

Fig. 2b - Geometry of three-dimensional collision trajectory: $V_T \sin\psi = V \cos\bar{\gamma} \sin(\psi - \bar{\chi})$.

4.1.2. First initial boundary-layer (E or V transition)

This boundary-layer connects the initial value E_0(resp. V_0) to the outer solution $\bar{E}_0$(resp. $\bar{V}_0$).

The equations are obtained by using the transformation $\tau = t/\varepsilon$ into (5) (6) (8) and by setting $\varepsilon = 0$.

The solution differs here according to the state variable set.

The analytic solution is given by:

a) Time-scale decomposition with E variable

$$\bar{\chi}_E = \bar{\chi}_0$$

$$\bar{h}_0 = arg\,\max_h \left\{V(F_M - D_0 - D_1)/(\bar{V}_0 - V)\right\}_{E=E\,current} \tag{14}$$

$$\bar{\gamma}_E = 0,\ \bar{\mu}_E = 0,\ \bar{n}_{zE} = 1$$

$$\bar{\lambda}_E = -(\bar{V}_0 - \bar{V}_E)/\{(\bar{V}_0 - V_T \cos\bar{\chi}_0)\bar{V}_E(F_m - D_0 - D_1)_{h=\bar{h}_E}\}$$

b) Time-scale decomposition with V variable

$$\bar{\chi}_V = \bar{\chi}_0$$

$$\bar{h}_V = arg\,\max_h\ V(F_M - D_0 - D_1)_{V=V\,current} \tag{15}$$

$$\bar{\gamma}_V = 0,\ \bar{\mu}_V = 0,\ \bar{n}_{zV} = 1$$

$$\bar{\lambda}_V = -(\bar{V}_0 - V)/\{(\bar{V}_0 - V_T \cos\bar{\chi}_0)(F_m - D_0 - D_1)_{h=\bar{h}_V}\}$$

In (14) and (15), the symbol $\bar{(.)}_E$ (resp. $\bar{(.)}_V$) denotes the first boundary-layer solution.

This $\bar{h}_E$ (resp. $\bar{h}_V$) profile is given in Fig 1 for a typical aircraft model. Let us notice that this figure does not show the original profile, computed from the relation (14) or (15), but a smoothed profile which is deduced from the original one by a classical polynomial profile which is deduced from the original one by a classical polynomial smoothing technique. It can be seen then that the discontinuity on altitude in transonic zone has been cancelled [7]. It turns out that this smoothing has no effect on degradation of performance of the aircraft, as can be shown in numerical simulation (section 5).

This $\bar{h}_E$ (resp. $\bar{h}_V$) profile is independent of the target characteristics, so it can be computed off-line and preregistered as a function of E (resp. V).

4.1.3. Second initial boundary-layer (χ transition)

The equations are obtained by using the transformation $\tau_2 = t/\varepsilon^2$ into (5) (6) (8) and by setting $\varepsilon = 0$.

The analytic zeroth-order solution is given by:

a) Time-scale decomposition with E variable

$$\bar{h}_\chi = arg\,\min_h \{H_{E0}(h,\chi) \times V/[2 - V^2D_1/(V^2D_1)_{h=\bar{h}_\chi}]\}$$

with:

$$H_{E0}(h,\chi) = [\bar{V}_0 - V\cos(\chi - \bar{\chi}_0)]/(\bar{V}_0 - V_T \cos\bar{\chi}_0)\ \ldots$$

$$\ldots + \bar{\lambda}_{E0} V(F_m - D_0 - D_1)] \tag{16}$$

$$\bar{\gamma}_\chi = 0$$

$$\bar{\lambda}_\chi = 2\,\bar{\lambda}_{E0}(V^2D_1)_{h=\bar{h}_\chi}\, tg\,\bar{\mu}_\chi$$

$$\bar{\mu}_\chi = sign(\bar{\chi}_0 - \chi).tan^{-1}\{H_{E0}(\bar{h}_\chi,\chi)/[-\bar{\lambda}_{E0}(VD_1)_{h=\bar{h}_\chi}]\}^{\frac{1}{2}}$$

$$\bar{n}_{z\chi} = 1/\cos\bar{\mu}_\chi$$

b) Time-scale decomposition with V variable

$$\bar{h}_\chi = arg\,\min_h \{H_{V0}(h,\chi)/[2 - D_1/(D_1)_{h=\bar{h}_\chi}]\}$$

with:

$$H_{V0}(h,\chi) = [\bar{V}_0 - V\cos(\chi - \bar{\chi}_0)]/(\bar{V}_0 - V_T \cos\bar{\chi}_0)\ \ldots$$

$$\ldots + \bar{\lambda}_{V0}(F_m - D_0 - D_1)] \tag{17}$$

$$\bar{\gamma}_\chi = 0$$

$$\bar{\lambda}_\chi = 2\,\bar{\lambda}_{V0}(VD_1)_{h=\bar{h}_\chi}\, tg\,\bar{\mu}_\chi$$

$$\bar{\mu}_\chi = sign(\bar{\chi}_0 - \chi).tan^{-1}\{H_{V0}(\bar{h}_\chi,\chi)/[-\bar{\lambda}_{V0}(D_1)_{h=\bar{h}_\chi}]\}^{\frac{1}{2}}$$

$$\bar{n}_{z\chi} = 1/\cos\bar{\mu}_\chi$$

In (16) and (17), the symbol $\bar{(.)}_\chi$ denotes this second boundary-layer solution on azimuth χ.

4.1.4. Third initial boundary-layer (h and γ transition)

For this initial boundary-layer, the symbol ($\hat{\cdot}$) is used. The equations are obtained by using the transformation $\tau_3 = t/\varepsilon^3$. By setting $\varepsilon = 0$, the first four equations in x, y, E or V, χ provide: $\hat{x} = x_0$, $\hat{y} = y_0$, $\hat{E} = E_0$ (or $\hat{V} = V_o$), $\hat{\chi} = \chi_o$ and the two other give:

$$
\begin{aligned}
d\hat{h}/d\tau_3 &= \hat{V} \sin \hat{\gamma} \\
d\hat{\gamma}/d\tau_3 &= (\hat{n}_z \cos \hat{\mu} - \sin \hat{\gamma})/\hat{V}
\end{aligned}
\tag{18}
$$

In this boundary-layer, the optimal control laws are given by

$$
\hat{n}_z, \hat{\mu} = \arg \min_{n_z, \mu} H(X, \lambda, n_z, \mu) \tag{19}
$$

where H is given by (7a) and x, y, E (or V), χ, λ_x, λ_y, λ_E (or λ_V), λ_χ variables are frozen at their initial values.

It can be noticed that this boundary-layer control problem (18) (19) is equivalent to the system (19) with the infinite-horizon performance index:

$$
\hat{J} = \int_o^\infty \left[1 + H_\chi(h, \gamma, n_z, \mu) \right] dt \tag{20}
$$

with $H_\chi(h, \gamma, n_z, \mu) = (\bar{V}_o - V \cos \gamma \cos(\chi_o - \bar{\chi}_o))/(\bar{V}_o - V_T \cos \bar{\chi}_o) \ldots$

$\ldots + \bar{\lambda}_{E_o} V(F_m - D_o - D_1 n_z^2) + \bar{\lambda}_{\chi o} n_z \sin \mu / V \cos \gamma$

To obtain zeroth-order feedback control laws for $\hat{n}_z$ and $\hat{\mu}$, the boundary-layer equations (18) (20) are linearized about the "outer" solution which is defined by the azimuth boundary-layer.

The linearization of (18) and (20) provides then:

$$
\begin{aligned}
\frac{d\delta y}{d\tau_3} &= A\, \delta y + B\, \delta u \\
\delta \hat{J} &= \int_o^\infty (\delta y^T\, \delta u^T) \begin{bmatrix} Q & S \\ S^T & R \end{bmatrix} \begin{pmatrix} \delta y \\ \delta u \end{pmatrix} d\tau_3
\end{aligned}
\tag{21}
$$

with:

$$
\delta y = \begin{vmatrix} h - \bar{h}_\chi \\ \gamma - \bar{\gamma}_\chi \end{vmatrix} \qquad \delta u = \begin{vmatrix} n_z - \bar{n}_{z\chi} \\ \mu - \bar{\mu}_\chi \end{vmatrix}
$$
$$
Q = \left(\frac{\partial^2 H}{\partial y^2} \right)_\chi \quad S = \left(\frac{\partial^2 H}{\partial y \partial u} \right)_\chi \;.\; R = \left(\frac{\partial^2 H}{\partial u^2} \right)_\chi \tag{22}
$$

The optimal control variable $\hat{n}_z$ and $\hat{\mu}$ for the linearized boundary-layer is given by the well-known solution of the quadratic linear infinite horizon problem:

$$
\delta \hat{u} = -R^{-1}(B^T P + S^T)\delta y \tag{23}
$$

where P is the non negative definite solution of the algebraic Riccati equation:

$$
P\hat{A} + \hat{A}^T + \hat{Q} - P B R^{-1} B^T P = 0 \tag{24}
$$

with $\hat{A} = A - B R^{-1} S^T$, $\hat{Q} = Q - S R^{-1} S^T$

For the zeroth-order boundary-layer problem, an analytical solution of Riccati equation can be obtained.

4.1.5. Final boundary-layer

For minimum-time interception, the final conditions on fast variables involve only altitude, to complete zeroth-order solution of the singularly perturbed optimal problem, we have to introduce only one final boundary-layer on the altitude and flight path angle variables.

For this purpose, the time-scale is stretched by using the transformation $\sigma_3 = (t_f - t)/\varepsilon^3$ in (5). The equations obtained have a similar form as for the initial boundary-layer equations (18) (20). The zeroth-order control $\tilde{u}$ for the final boundary-layer control is obtained by linearizing the equations about the outer solution, given by (13). The asymptotic stability is obtained by a backwards integration and thus the linearized optimal control is given by (23) with the non-positive definite solution N of the algebraic Riccati equation (24).

4.2. Final control law

In order to achieve final interception condition on altitude, the final control is obtained by using the following approaches:

1) The final flight path is first computed by a backwards integration of the complete motion equations (5), with the control defined as above for the final boundary-layer, from final conditions up to the outer-solution. The obtained flight path is then stored and a simple guidance control law is used, in direct time, to follow the stored flight path.
The computation of unknown final state variables, for backwards integration, is described below.

2) An other technique for final control is to apply a three-dimensional collision-type control law when the relative range to the target becomes below a specified value. The geometry of such a three-dimensional collision trajectory is shown in fig. 2b.

Computation of unknown final state variables (short-range intercept)

The statement is described, as previously, for the first set of state variables (with E), the application to the second set can be done straightforwardly.

For minimum-time interception, the following final variables are fixed : $x_f = y_f = 0$, $h_f = h_T$. For the remaining state variables (χ, γ), their final values are given by the outer-solution, that is: $E_f = \bar{E}_o$, $\chi_f = \bar{\chi}_o$, $\gamma_f = \bar{\gamma}_o = 0$.

Nevertheless, it can be noticed that, for short-range or medium range interception-trajectories, the flight-time is not longer enough so that the outer solution, defined by $\bar{E}_o$, cannot be reached.

In order to take into account short-range trajectories, the final conditions E_f, χ_f and γ_f are computed by writing that the total relative distance, which is covered from initial position to final interception, is equal to variation of energy level from its initial value E_0 to the final value E_f.

The total relative distance to be covered is defined as the sum of relative horizontal distance and the final climb (or dive) from altitude given by outer-solution $\bar{h}_E(E)$ to the target altitude. The trajectory is assumed to be of collision-type for each of both phases.

With the above assumptions, the final conditions E_f, χ_f and γ_f are given by the relations:

$$x_f - x_o = -x_o = \int_{E_o}^{E_1} \frac{V\cos\chi - V_T}{V\left[F_m - D_o - D_1 n_z^2\right]_{\bar{h}_E(E)}} dE = \phi_x[E_1, \chi_f]$$

$$y_f - y_o = -y_o = \int_{E_o}^{E_1} \frac{V\sin\chi}{V\left[F_m - D_o - D_1 n_z^2\right]_{\bar{h}_E}} dE = \phi_y[E_1, \chi_f] \tag{25}$$

$$h_T - \bar{h}_E(E_1) = \int_{E_o}^{E_f} \frac{\sqrt{V^2 - V_T^2}}{V\left[F_m - D_o - D_1 n_z^2\right]_{\bar{h}_E}} dE \ldots$$

$$\ldots = \phi_h[E_1, E_f], \quad \cos\gamma_f = \frac{V_T}{V_f}$$

4.3. First-order SPT correction

It can be seen in numerical examples that the zeroth-order solution, given by boundary-layer control (22) (23), is unable to follow the energy-climb profile $\bar{h}_E(E)$ (or $\bar{h}_V(V)$), because the nominal flight-path angle γ_χ is identically zero. The real flight path angle is undoubtedly different from zero, since altitude changes in the energy climb profile (see Fig. 1). To improve the accuracy of the control law, first-order asymptotic expansions could be performed for the outer-solution. Nevertheless, we adopt here a small correction term which has been successfully used in a previous study[7]. The zeroth-order boundary-layer control (22) (23) is still used, but the nominal value $\bar{\gamma}_\chi$ is replaced by its first-order asymptotic expansion term which can be written in the form:

$$\bar{\gamma}_{\chi_1} = \frac{1}{V} \cdot \left(\frac{d\bar{h}_E}{dE} \right) \times \dot{E} \tag{26}$$

where the (dh_E/dE) term can be computed easily by numerical differentiation along the $\bar{h}_E$ profile (see Fig. 1).

4.4. Summary of the closed-loop guidance law

A closed-loop guidance law, valid for a large flight envelope three-dimensional interception is obtained by using SPT with some further improvements which have been proposed in order to achieve the final conditions of interception where the original SPT fails.

The closed-loop control law requires the following step of calculations (as previously stated, the solution is related to the first set of state variables, the statement with the second set is similar to the first one):

1) Outer altitude profile $\bar{h}_E(E)$ (see (14)).
2) Final values E_f, χ_f, γ_f (see (25)).
3) First boundary-layer altitude profile $\bar{h}_\chi(E)$ (see (16)).
4) "Nominal" values of controls $\bar{\mu}_\chi$, $\bar{n}_z$ defined by (16).
5) Closed-loop control given by (22) (23) (24) (26).
6) Change from previous control to final control can be performed very simply: it is obtained by changing nominal value of $\bar{\gamma}_\chi$ and $\bar{\mu}_\chi$, when $E \geq E_1$ (see (25)), by the values obtained from three-dimensional collision trajectory geometry, given in fig. 2b.

5. Numerical results

Numerical results have been performed with the closed-loop obtained, by using the two sets of state variables described above.

The solutions obtained with both control laws are defined respectively by SPE for the control related to the first set (that is with E variable), and by SPV for those related to the second set (with V variable).

In numerical simulations, the target trajectory is assumed to be a level flight with constant speed and constant altitude ($V_T = 200$ m/s, $h_T = 12000$ m).

Several initial conditions have been considered for the aircraft including high and low altitude, with large offset of line-of-sight.

In all the considered cases, approximate closed-loop control laws provided very accurate final interception conditions, the final relative range to the target remains below 100 m.

Those solutions have also been compared with the optimal exact numerical solutions which are given in an open-loop form by a projected gradient algorithm. This last technique allows to fulfil all the constraints of the optimal atmospheric flight paths, given by (3), by using multiple adjoint vectors[9].

In comparison with the optimal exact solution, both the closed-loop control laws (SPE and SPV) provide a better than 4% accuracy on the time of intercept as shown in Table 1.

6. Conclusion

Sub-optimal guidance laws have been developed in this paper for three-dimensional interception manoeuvers. The technique used is derived from singular perturbation theory. In opposite with many studies on this subject, a realistic time scale separation has been used with two sets of state variables, where altitude and flight path angle are simultaneously treated in a same time scale. A closed-loop control law has been obtained by linearizing the boundary-layer equations about the "outer" solution defined by an energy-climb profile or velocity-climb profile.

With the expedient of "control reset" whereby each current instant is taken as an initial time, and with convergence properties of boundary-layers, the control laws apply everywhere, with the exception of a vicinity of the final time when terminal condition on altitude is specified.

To satisfy this constraint, the control law is switched to a linear feedback guidance mode about a stored trajectory in the neighbourhood of the terminal state. This latter trajectory is computed off-line by backward integration of dynamic equations with the suboptimal closed-loop control obtained as above.

These sub-optimal laws have been compared, in numerical simulations, with the exact open loop solutions, obtained from an iterative numerical method based upon a projected-gradient technique. In most examples, a better than 4% accuracy was obtained for the performance index. The computation time is very small, and is compatible with real-time on-board computer applications.

TABLE 1 COMPARISON BETWEEN SEVERAL SOLUTIONS FOR MINIMUM-TIME INTERCEPTION

Main parameters

t_f = interception time
d_f = relative distance to the target at t_f
γ_f = terminal flight path angle of the interceptor.

Abbreviations

SPE: singular perturbation with E-transition first boundary-layer solution
SPV: singular perturbation with V-transition first boundary-layer solution
gradient: optimal solution obtained by a projected-gradient technique

Target	Altitude $h_T = 12000$ m; velocity $V_T = 200$ m/s														
Interception type	Vertical plane			Three-dimensional											
	High altitude interception												Low altitude interception		
Initial aircraft conditions $\Delta x_0 (m)$	25000			25000			15000			10000			20000		
$\Delta y_0 (m)$	0			5000			0			0			0		
$h_0 (m)$	12000			10000			10000			10000			2000		
V_0 (m/s)	313			300			300			300			300		
χ_0 (°)	0			0			-90			-179			-90		
γ_0 (°)	0			0			0			0			0		
Final parameters	t_f (s)	d_f (m)	γ_f (°)	t_f (s)	t_f (m)	γ_f (°)	t_f (s)	d_f (m)	γ_f (°)	t_f (s)	d_f (m)	γ_f (°)	t_f (s)	d_f (m)	γ_f (°)
Optimal solution (gradient)	96.5	3	22	102	5	20.5	88	33	32	105.4	9.7	31	123.5	7	40
SPE solution	98.5	34	10.8	104.6	49	5.8	89.7	33	16.9	107.2	57	17.3	127.7	17	24.8
SPV solution	99.1	11	14.3	103.6	14	11.3	91.3	27	14.6	105.5	27	25	128.1	8	26.3
Figure n°	3			4			5			6			7		

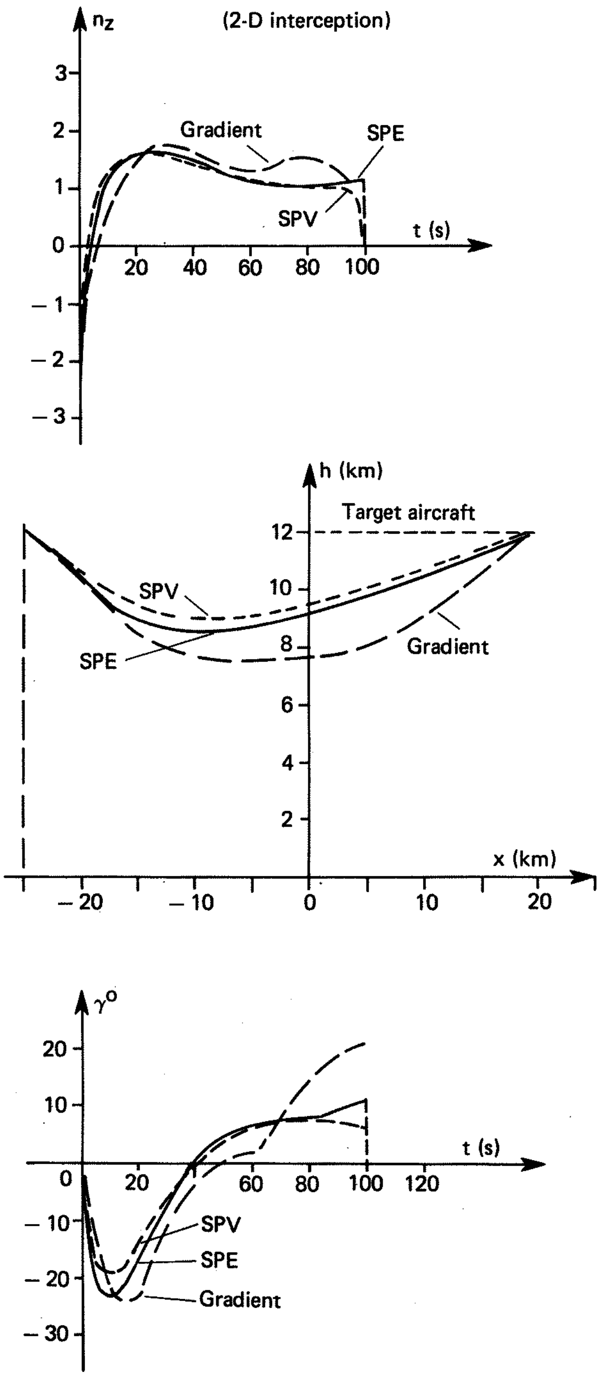

Fig. 3 - Minimum-time to intercept (Interceptor $V_0 = 313$ m/s).

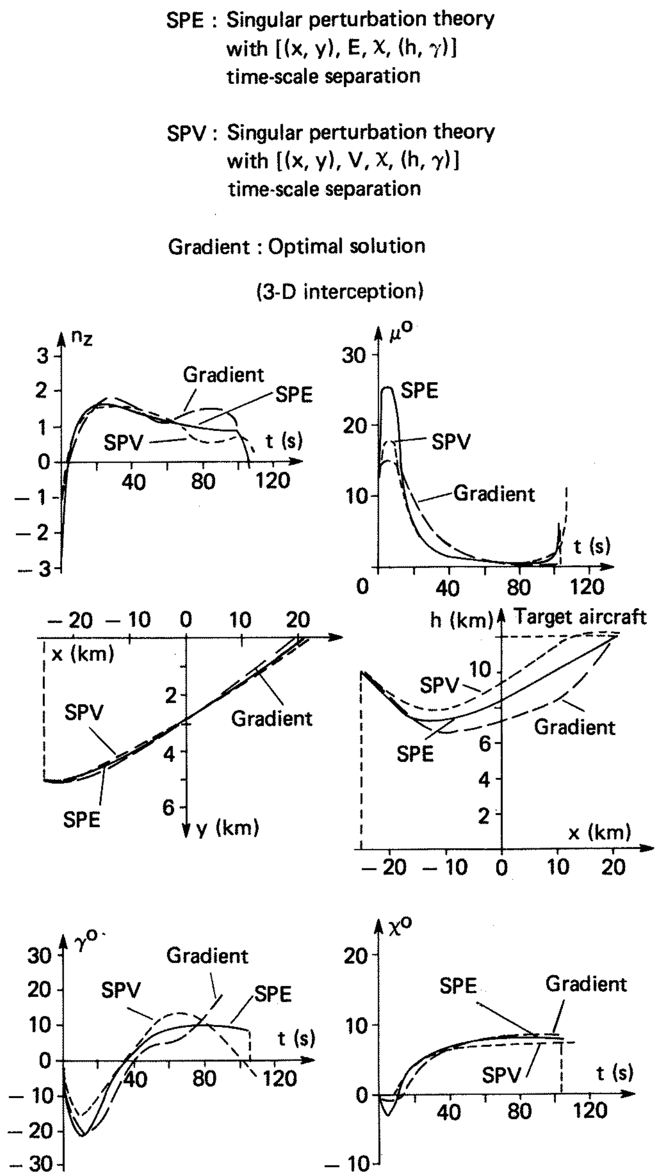

Fig. 4 - Minimum-time to intercept (Interceptor $V_0 = 300$ m/s).

(3-D interception)

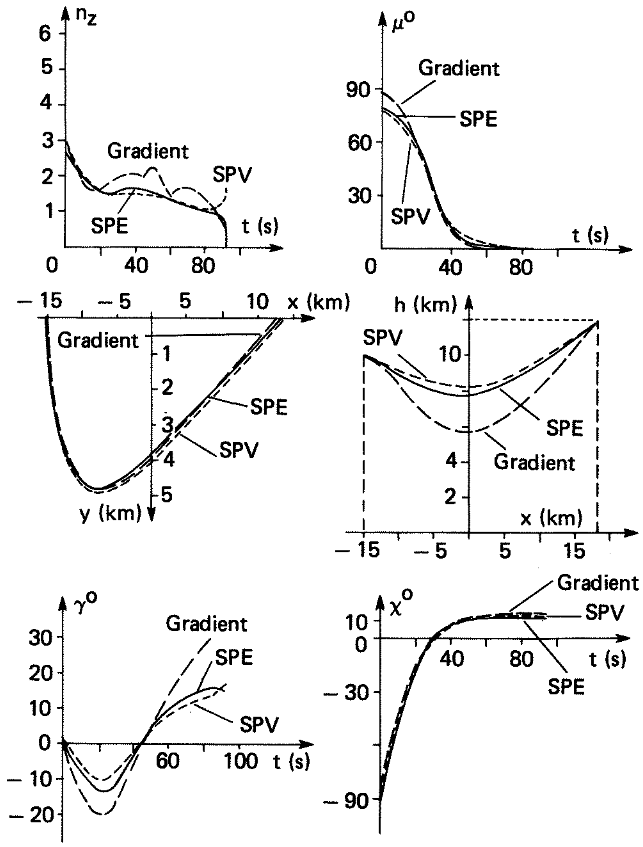

SPE : SPT with E variable
SPV : SPT with V variable
Gradient : Optimal solution

Fig. 5 - Minimum-time to intercept (Interceptor V_o = 300 m/s).

(3-D interception)

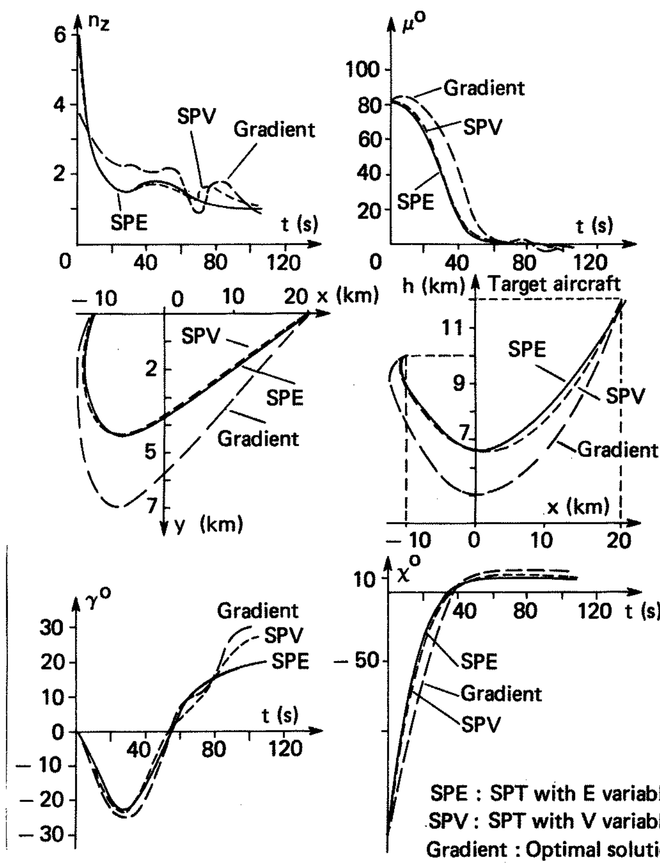

SPE : SPT with E variable
SPV : SPT with V variable
Gradient : Optimal solution

Fig. 6 - Minimum-time to intercept (Interceptor V_o = 300 m/s, χ_o = - 179°).

(3-D interception)

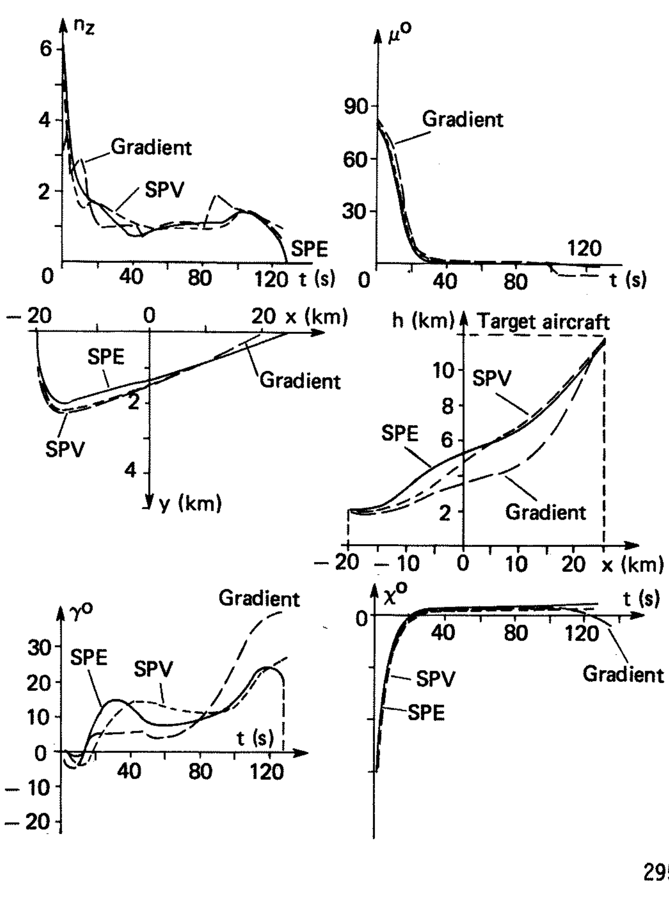

SPE : Singular perturbation theory with [(x, y), E, X, (h, γ)] time-scale separation

SPV : Singular perturbation theory with [(x, y), E, X, (h, γ)] time-scale separation

Gradient : Optimal solution

Fig. 7 - Minimum-time to intercept (Interceptor V_o = 300 m/s).

References

1. SHINAR J., ROTSZTEIN Y. and BEZNER E.: "Analysis of Three-Dimensional Optimal Evasion with Linearized Kinematics", J. of Guidance and Control, Vol. 1, Sept.-Oct. 1979, pp. 353-360.

2. CALISE A.J.: "Singular Perturbation Techniques for On-Line Optimal Flight Path Control", J. of Guidance and Control, Vol. 4, n° 4, July-August 1981, pp. 398-405.

3. NEGRIN M. and SHINAR J.: "Solution of Three-Dimensional Interception by Inclined Plane using the Forced Singular Perturbation Technique", 24th Israel Annual Conference on Aviation and Astronautics, Haifa, Feb. 1982.

4. PRICE D.B., CALISE A.J. and MOERDER D.D..: "Piloted Simulation of an On-Board Trajectory Optimization Algorithm", J. of Guidance and Control, Vol. 7, n° 3, May-June 1984, pp. 355-360.

5. SHINAR J., WELL K.H. and JARMACK B.: "Near-Optimal Feedback Control for Three-Dimensional Interception", 15th ICAS Congress London, U.K., Sept. 1986.

6. FUMIAKI IMADO and SUSUMU MIWA: "Three-Dimensional Study for Evasive Manoeuvers of a Fighter against a Missile", AIAA 86-2038, pp. 957-966.

7. HUYNH H.T. and MOREIGNE O.: "Quasi-Optimal On-Line Guidance Laws for Military Aircraft", AIAA Guidance and Control Conference, Snowmass, Colorado (USA), 19-21 August 1985.

8. RALSTON A. and WILF H.S.: "Mathematical Methods for Digital Computers", Vol. 2, 1967, pp. 171-184.

9. AUMASSON C., LANDIECH Ph. : "Méthode de gradient projeté généralisé pour l'optimisation numérique de trajectoires", ONERA Technical Report n° 22/6115 SY, 1987.

10. ARDEMA M.: "Singular Pertubations in Systems and Control", International Center for Mechanical Sciences, NASA Ames Research Center, Springer-Verlag, 1983.